2010 21st International Lightning Detection Conference
19 – 20 April • Orlando, Florida, USA
3rd International Lightning Meteorology Conference
21 – 22 April • Orlando, Florida, USA

LIGHTNING ACTIVITY AND CHARGE STRUCTURE OF MICROBURST PRODUCING STORMS

Kristin M. Kuhlman, Travis M. Smith
Cooperative Institute for Mesoscale Meteorological Studies, University of Oklahoma and
NOAA/National Severe Storms Laboratory, Norman, OK, USA

Steven T. Irwin
School of Meteorology, University of Oklahoma, Norman, OK, USA and
Cooperative Institute for Mesoscale Meteorological Studies, University of Oklahoma

1. Introduction

Microbursts are cause for concern for forecasters because of their rapid onset and noted relevance for aircraft safety. Many studies have evaluated the typical environmental profiles for days which microburst are likely to occur, but it is difficult for a forecaster to anticipate which storm in particular will produce a microburst. While radar remains the number one tool for forecasters evaluating storms, lightning data may be able to provide additional clues due to the inherent links of charge generation to storm updraft and ice microphysics.

While prior work linking lightning rate to severe microbursts depicts a rapid increase in the flash rate with sharp decline thereafter (Goodman et al, 1988; Williams et al, 1999), a combination of phased array radar (PAR), lightning mapping array (LMA) and Vaisala National Lightning Detection Network data will be used in this study to help provide a physical understanding how three-dimensional lightning data may be used by forecasters for microburst prediction. Due to the rapid updates and high spatial resolution of both the PAR and LMA, both of these systems are able to capture the quick generation and evolution of microbursts.

This study examines 8 different storms in central Oklahoma producing microbursts to determine what charge structure, lightning rate, flash size and location, and initiation heights may signal differences from non-microburst producing storms and which of these factors may act as a signature or precursor to a microburst.

2. Data and Methodology

The main radar employed in this study is the National Weather Radar Testbed Phased Array Radar (PAR). The PAR is a research radar that collects data from a 9.4-cm-wavelength, single-faced, phased-array antenna that forms a beam electronically by controlling the phases of multiple transmit-receive elements (Zrnic´ et al. 2007; Heinselman et al. 2008). The radar volumetrically scans storms at time scales of seconds instead of several minutes (when compared to WSR-88D radars) and is capable of variable scanning strategies including multiple low-level scans within a full volumetric scan. The current design is single-faced (instead of 4-faced) so it is only capable of scanning a 90 degree sector while stationary (instead of full 360 degree sectors).

The Oklahoma LMA (Thomas et al. 2004; MacGorman et al. 2008) is a Global Positioning System (GPS) based, time of arrival system, that maps lightning by measuring the time at which an electro-magnetic signal produced by a developing lightning channel arrives at each station in the array in central Oklahoma. Individual

flashes mapped by the LMA can be analyzed to infer the regions of storm charge involved in a flash. According to the bi-directional model (Mazur and Ruhnke 1993), which has become the paradigm for understanding lightning development, lightning is initiated between regions of opposite charge where the magnitudes of the electric field are near a local maximum. The lightning then propagates into regions of opposite charge, with the negative leader traveling toward regions of positive charge and the positive leader traveling toward regions of negative charge.

Shao and Krehbiel (1996) and Rison et al. (1999) have demonstrated that VHF mapping systems such as the LMA preferentially map negative leaders (which tend to propagate through positive charge), as negative leaders produce much more noise at the radio frequencies used by the LMA than positive leaders do. Thus, individual flashes can be examined to identify the charge structure of the storm (Wiens et al. 2005). This method requires a flash-by-flash analysis, subjectively determining the first several sources and higher density activity (positive charge) from the sources occurring later and at lower density (negative charge).

The cloud-to-ground lightning data used in this study was collected by the Vaisala National Lightning Detection Network (NLDN). The NLDN consists of over 100 ground-based sensing stations located across North America that detect electromagnetic signals from lightning channels to ground (Cummins et al. 1998).

The Warning Decision Support System – Integrated Information (WDSS-II) is the second generation of a system of tools for the analysis, diagnosis and visualization of remotely sensed weather data (Lakshmanan et al 2007). WDSS-II provides the algorithm infrastructure and interface for examining the combination of sensors used in this study, including a newly adapted lightning flash and segmotion storm tracking algorithms (Lakshmanan et al 2009).

3. Results

As mentioned in the introduction, multiple storms producing microbursts across various days in central Oklahoma have been examined. They are broken down by date in the sections below.

a. 9-10 July 2007

Numerous multicell clusters developed over the Oklahoma and southern plains region associated with a short wave trough moving through the area, providing moderate instability and weak mid-level shear. Interaction between storm outflows provided temporary updraft intensification prior to the numerous downbursts seen throughout the evening. Three separate microbursts occurring with three separate storms are investigated here.

All of the storms investigated on this day contained a normal polarity charge structure, with the bulk of the lightning occurring between an upper positive and mid-level negative charge region (Fig. 3.1). Prior to the first microburst at 2252, the storm exhibited quick growth of both the 45-50 dBZ core and LMA activity, expanding in size and height to above 15 km. Lightning activity increased between the lowest two charge regions during and after the microburst (2250-2300 UTC); it is during this time there is also a marked increase in the -CG rate from the cluster (Fig. 3.2). Similarly, the microburst occurring at 0003 UTC occurs with a region of a storm cluster that, prior to 2353, the majority of lightning was contained between 7-12 km. The next 10 min

depicts a rapid increase in LMA sources throughout the column as well as an increase in the total flash rate (Fig. 3.2) before the merger of cells within the cluster at 0007 UTC.

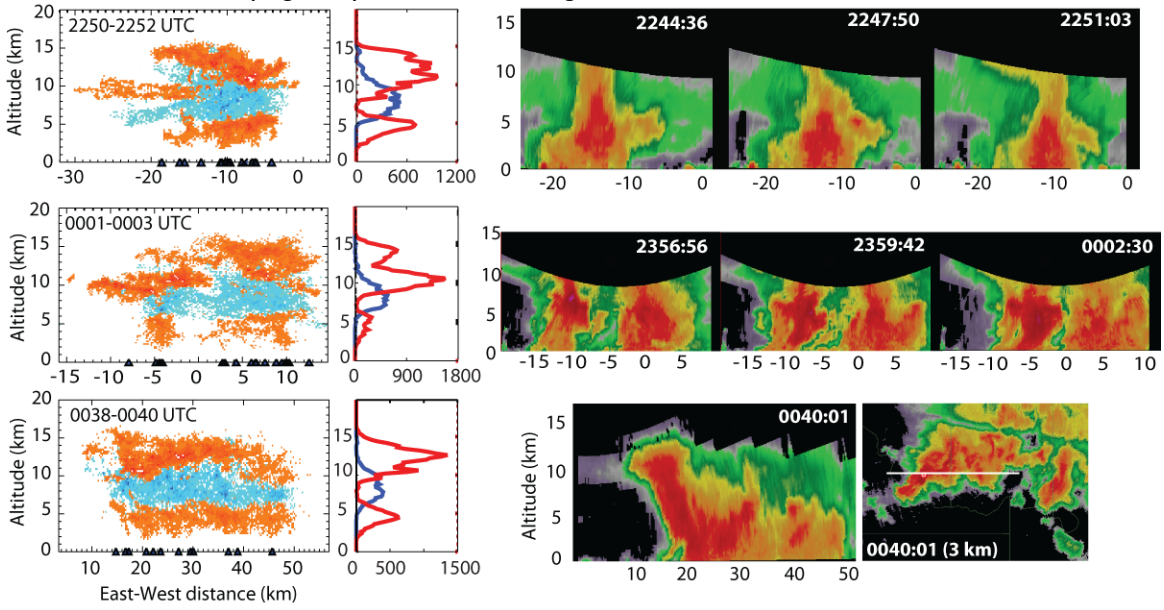

Figure 3.1: (Left) Charge structure and histograms of the storms at the time of the microburst. Charge structure determined by LMA analysis, positive charge (orange) and negative charge (blue). CG locations from NDLN indicated by black triangles. Height histogram of number of LMA points, separated according to charge. (Right) Corresponding reflectivity slice along core of storm from phased array radar just prior and at the time of microburst (times indicated on all plots).

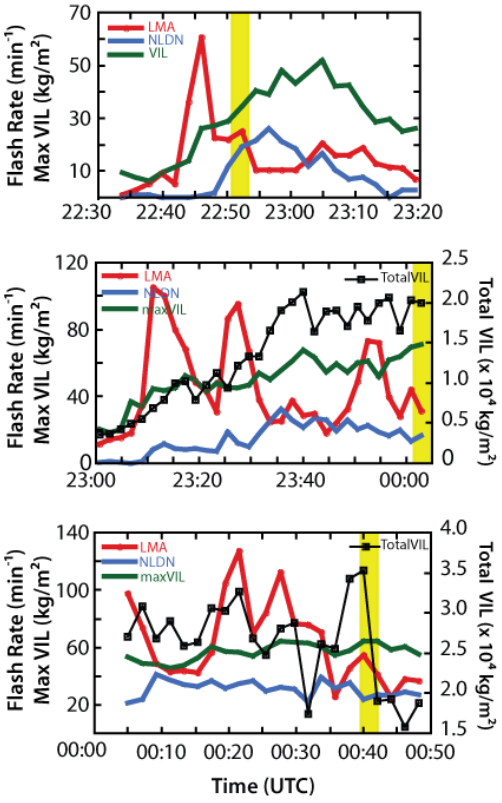

Figure 3.2: Time series plots of total flash rate from LMA (red), CG rate from NLDN (blue), maximum VIL values from PAR (green) for the three microbursts (time highlighted in yellow) occurring on 9-10 Jul 2007.

Lightning activity in the case of the third microburst is slightly different, as all three charge layers were very active before, during and post-microburst and the cluster contained the highest average -CG of the three storm clusters (Fig. 3.2). There is a slight jump in the total flash rate occurring just at the time of the microburst and a large increase in the Total VIL for the storm indicative of the increase in reflectivity with the storm, particularly above 12 km occurring around 0032 UTC.

b. 24 July 2007

This short-lived storm produced a microburst just after 2130 UTC (Fig. 3.3). No lightning was observed before 2125 UTC with the storm and no lightning was observed after 2135 UTC following the microburst. The decent of lightning activity corresponded directly with the decent of core in reflectivity from PAR data. At the point of the microburst, lightning was predominately initiating between

a mid-level negative charge and lower positive and there was a noted

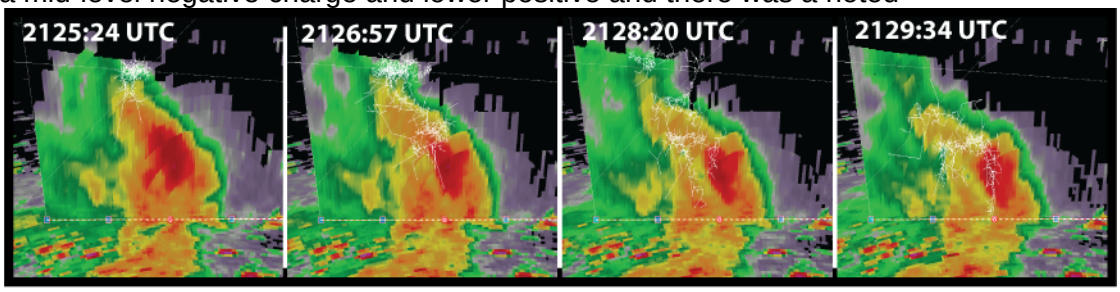

Figure 3.3: Reflectivity cross-sections through core of storm from phased array radar just prior to and at the time of microburst (times indicated on plots). Lightning leaders for individual flashes from LMA overlaid in white.

increase in -CG activity. Prior to 2127, the storm produced no CG activity and all lightning was contained between the upper-positive and mid-level negative charge regions.

c. 29 August 2008

Multiple small pulse-type storm clusters developed in the region due to strong instability, but low shear conditions. Storm A produced two microbursts in less than 20 min (Fig. 3.4A). The first occurred at the time of the collapse of the first updraft pulse on the SE side. A new, stronger updraft then developed quickly on the SW side, lofting 30 dBZ reflectivities to 11 km and with increasing lightning activity peaking around 2242 UTC, before expanding through the column with a second microburst occurring at 2251 UTC.

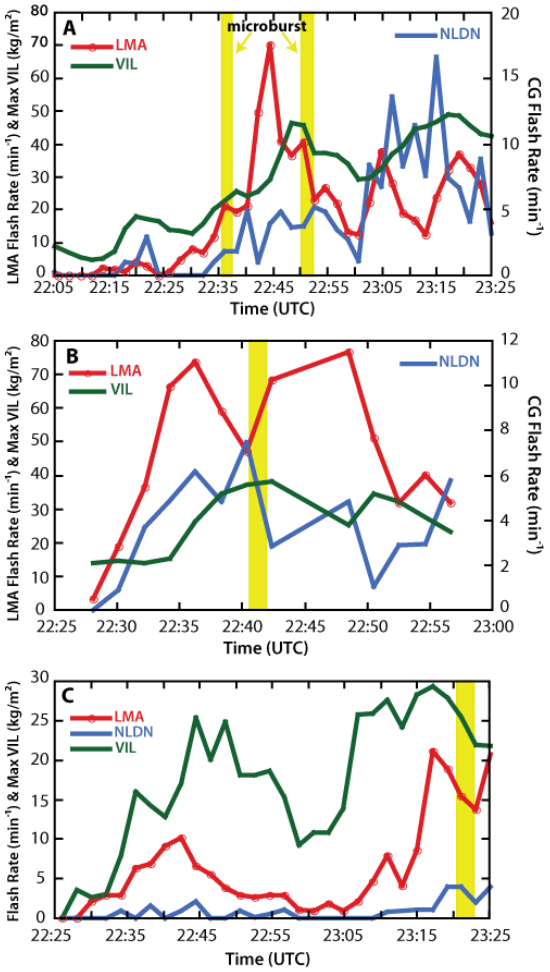

Figure 3.4: Same as Fig. 3.2, except for 29 Aug 2008. Each time series represents a different storm occuring within the PAR scanning area.

The two other storms producing microbursts on this day displayed "lightning jumps" in the 5 to 10 min prior to the microburst. Flash rates for storm B quickly reached 75 flashes per min before falling to near 50 at the time of the microburst, meanwhile the CG rate increased over the 10 min period from near 7 –CG flashes per min(Fig. 3.4B). Storm C contained much lower flashes rates, but did also contain a jump in total flash rate from near 5 per min ten min prior to 20 per min 5 min before the microburst (Fig. 3.4C).

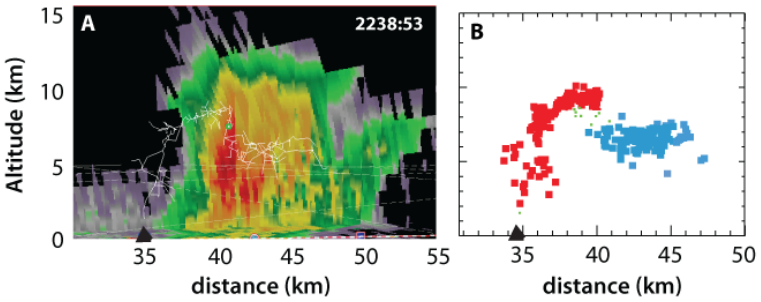

Figure 3.5: (a) Cross-section of reflectivity and lightning activity at 2238:53 UTC on 29 Aug 2008. Location of lightning initiation point highlighted by green dot, location of NLDN ground detection by black triangle. (b) LMA points associated with flash analyzed by charge (positive-red, negative-blue).

Not all -CG activity on this day initiated between the mid-negative and lower positive regions. On this day, three separate -CG flashes ("bolts from the blue") initiated between the upper positive and mid-level negative charge regions (Fig. 3.5).

d. 30 June 2009

A stalled cold front combined with moderate instability allowed for convection to develop throughout central Oklahoma on 30 Jun 2009. Steep lapse rates and a large temperature-dewpoint difference contributed to the possiblity of downburst-producing storms. The same multicell cluster produced two separate microbursts in Oklahoma County within a 30 min period. The first microburst was associated with the northern area of the cluster with the first lightning and 35 dBZ reflectivity occurring simultaneously at 2204 UTC. The storm quickly intensified with a large jump in flash rate and reflectivity occurring at the time just prior to the microburst before the cell merges with the larger storm cluster to the south. The second microburst occurred at 2251 UTC, associated with the same storm cluster on SW side coincident with a region of peak initiation rate of lightning and also peak reflectivity. The CG activity in the storm cluster remained focused around the area of the microburst, all negative polarity.

In this case, the storm cluster exhibits a definite lightning jump in both total flash rate and CG flash rate just prior or during (CG) the microburst. Both the PAR and LMA data clearly show an increase in intensity in the region of the cell immediately prior to the microburst, however only in the 3-5 minutes prior.

4. Discussion and Conclusions

Consistently, all storms producing microbursts in this study contained a normal tripole charge structure. Though there is not always a definite "lightning jump" associated with each downburst, there does seem to be some typical lightning behavior within these storms. Generally, prior to the time of the downburst, lightning

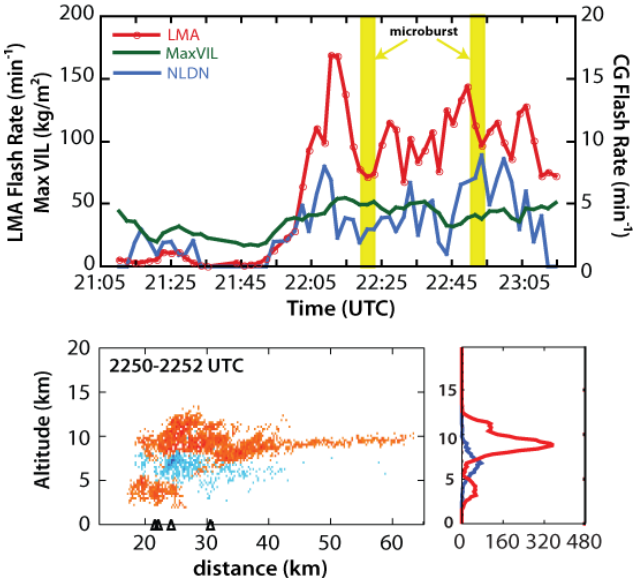

Figure 3.6: (top) Time series plot of flash rate and VIL (see Fig. 3.2) and (bottom) charge structure and histogram of LMA points at time of second microburst (see Fig. 3.1).

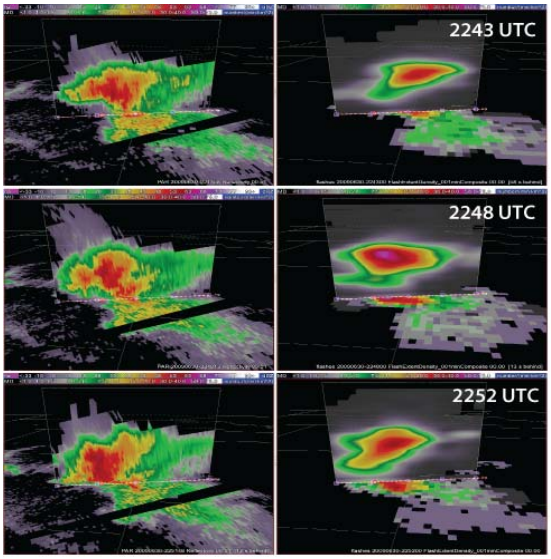

Figure 3.7: (left) 3D view at radar reflectivity from PAR. (right) 3D view of lightning from LMA (color scale represents number of points) prior to and at time of second microburst by this storm on 30 Jun 2009.

occurred between the upper two charge regions. Lightning activity has a noted increase between the lowest two charge regions in sync with the decent of the reflectivity core immediately before the microburst. Lightning flashes initiated between this mid-level negative and lower positive region at this time almost always involves -CG strike (>80% of the time on 29 Aug 2008) and all events studied typically show a increase in the –CG rate at the time of the microburst.

5. References

Cummins, K., M. Murph, E. Bardo, W. Hiscox, R. Pyle, and A. Pifer, 1998: A combined TOA/MDF technology upgrade of the U.S. National Lightning Detection Network. *J. Geophys. Res*., 103, 9035–9044.

Goodman, S.J., Buechler, D.E., Wright, P.D., Rust, W.D., 1988. Lightning and precipitation history of a microburst-producing storm. *Geophys. Res. Lett.* 15, 1185 – 1188.

Heinselman, P. L., D. L. Priegnitz, K. L. Manross, T. M. Smith, and R. W. Adams, 2008. Rapid Sampling of Severe Storms by the National Weather Radar Testbed Phased Array Radar. *Weather and Forecasting*, *23*(5), 808. doi: 10.1175/2008WAF2007071.1.

Lakshmanan, V., T. Smith, G. Stumpf, and K. Hondl, 2007. The Warning Decision Support System–Integrated Information. *Weather and Forecasting*, *22*(3), 596. doi: 10.1175/WAF1009.1.

Lakshmanan, V., K. Hondl, and R. Rabin, 2009: An efficient, general-purpose technique for identifying storm cells in geospatial images. *J. Ocean. Atmos. Tech.,* 26 (3), 523–37.

MacGorman, D. R., and Coauthors, 2008: TELEX: The thunderstorm electrification and lightning experiment. *Bull. Amer. Meteor. Soc.*, 89, 9971013.

Mazur, V. and L. Ruhnke, 1993: Common physical processes in natural and artificially triggered lightning. *J. Geophys. Res*., 98, 913–930.

Shao, X. M. and P. R. Krehbiel, 1996: The spatial and temporal development of intracloud lightning. *J. Geophys. Res*., 101, 26641–26668.

Thomas, R., P. Krehbiel, W. Rison, S. Hunyady, W. Winn, T. Hamlin, and J. Harlin, 2004: Accuracy of the lightning mapping array. *J. Geophys. Res*., 109, doi:10.1029/2004JD004549.

Wiens, K. C., S. A. Rutledge, and S. A. Tessendorf, 2005: The 29 June 2000 supercell observed during STEPS. Part 2: Lightning and charge structure. *J. Atmos. Sci.,* 62, 4151–4177.

Williams, E., B. Boldi, A. Matlin, M. Weber, S. Hodanish, Sharp, D., et al. (1999). The behavior of total lightning activity in severe Florida thunderstorms. *Atmos. Res*.

Zrnic´, D. S., and Coauthors, 2007: Agile-beam phased array radar for weather observations. *Bull. Amer. Meteor. Soc*., 88, 1753– 1766.